

## Tailoring the morphology and electrocatalytic properties of electrochemically formed Ag/TiO<sub>2</sub> composite deposits on titanium surfaces

S. V. MENTUS<sup>1\*#</sup>, I. BOŠKOVIĆ<sup>2</sup>, J. M. PJEŠČIĆ<sup>2</sup>, V. GRUDIĆ<sup>2</sup> and Ž. BOGDANOV<sup>3</sup>

<sup>1</sup>Faculty of Physical Chemistry, University of Belgrade, Studentski trg 16, 11000 Belgrade, Serbia,

<sup>2</sup>Faculty of Metallurgy and Technology, Podgorica University, 81000 Podgorica, Montenegro and

<sup>3</sup>Vinča Institute of Nuclear Sciences, 11001 Belgrade, Serbia

(Received 14 May 2007)

**Abstract:** Three different forms of Ag/TiO<sub>2</sub> composite layers, which have whisker-, dot- and island-like distribution of silver were obtained on a mechanically polished titanium surface by adjusting the conditions of silver deposition from an aqueous AgNO<sub>3</sub> solution. The deposit morphology was the result of both the program of electrode polarization and the template action of the simultaneously formed TiO<sub>2</sub> layer. The catalytic activity of the composite layers toward the oxygen reduction reaction was studied in aqueous 0.1 M NaOH solutions and found to be a function of both the surface loading of silver and the type of silver distribution within the Ag/TiO<sub>2</sub> composite layers. The reaction path of oxygen reduction on the composite layers was found to be always a 4e<sup>-</sup> one, characteristic otherwise of polycrystalline silver electrodes.

**Keywords:** metal/oxide composite electrocatalysts, oxygen reduction reaction, rotating disc electrode, silver electrodeposition, titanium dioxide film.

### INTRODUCTION

Heterogeneous systems consisting of small metal particles dispersed on electronic conductor, semiconductor and ionic conductor supports, display a number of interesting properties of both fundamental and applicative significance. By dispersing catalytically active metal over a high-surface-area support, its utilization may be enhanced simply based on the increase of the real surface area on which an electrochemical process, otherwise heterogeneous in nature, occurs. Metal–semiconductor heterogeneous systems are of significant interest in optics, electrophysics, catalysis, *etc.*<sup>1</sup> On going to nano-dispersions, quite new effects, characteristic of individual atoms, may also be experienced. For instance, Ng *et al.*<sup>2</sup> investigated the particular electrochemical behaviour of nano-dispersed sil-

\* Corresponding author. E-mail: slavko@ffh.bg.ac.yu

# Serbian Chemical Society member.

doi: 10.2298/JSC0712403M

ver on carbon black, manifested as both a cathodic shift of the equilibrium potential and an aggravated anodic dissolution.

Polycrystalline silver shows a high catalytic effectiveness in electrochemical oxygen reduction in alkaline solutions.<sup>3</sup> McIntyre *et al.*<sup>4</sup> evidenced a four-electron reduction mechanism of oxygen reduction on all silver crystallographic planes in alkaline solutions. Following this knowledge, Hacker *et al.*<sup>5</sup> and Yang *et al.*<sup>6,7</sup> investigated the oxygen reduction reaction in alkaline solutions using nano-dispersed silver supported by carbon nano-fibres<sup>5</sup> and carbon black.<sup>6,7</sup> Chatelet *et al.* compared the catalytic effectiveness of carbon-supported silver<sup>8</sup> and bimetallic silver-platinum<sup>9</sup> catalysts with that of pure bulk platinum. Carbon supported silver was proposed to replace carbon supported platinum as the cathode material in fuel cells, metal-air batteries<sup>10</sup> and electrolyzers for chlorine production.<sup>11</sup>

High surface area is not a unique benefit of supported metal catalysts in electrocatalysis. Another one may be the so-called strong metal-support interaction (SMSI), which enhances the catalytic effectiveness of a catalytically active metal. This effect was observed in systems of noble metals supported by reducible VIII group metal oxides, primarily TiO<sub>2</sub>.<sup>12-19</sup>

The metal oxide films were synthesized preferably by thermal decomposition of thermodegradable compounds of titanium and catalytically active metals. Beer,<sup>20</sup> for instance, applied a RuO<sub>2</sub> coating on a Ti surface by thermal decomposition of RuCl<sub>3</sub>. Haruta *et al.*<sup>16-18,21</sup> evidenced high catalytic effectiveness of a nano-Au/TiO<sub>2</sub> composite catalyst for CO oxidation at low temperatures, although each of the components alone is catalytically ineffective. This finding was given as an example of the SMSI effect. These authors prepared the catalyst by precipitation of Au(III)-hydroxide onto TiO<sub>2</sub> powder, with the subsequent reduction of the Au hydroxide by heating in a hydrogen atmosphere. Burrows *et al.*,<sup>22</sup> Kuhn *et al.*,<sup>23</sup> Kalinovski *et al.*<sup>24</sup> and Erenberg *et al.*<sup>25</sup> synthesized RuO<sub>2</sub>-TiO<sub>2</sub> and RuO<sub>2</sub>-TiO<sub>2</sub>-IrO<sub>2</sub> layers on a Ti surface, known as effective composite catalysts in the oxidation of chloride. Some papers describe electrochemical procedures to deposit catalytically active metal on titanium. For instance, Vuković *et al.*<sup>26-28</sup> deposited noble metals and their alloys on a titanium surface galvanostatically and obtained very developed deposits. Mentus<sup>29</sup> deposited a Pt/TiO<sub>2</sub> layer potentiodynamically and outlined the template action of TiO<sub>2</sub>. Emery *et al.*<sup>30</sup> studied the kinetics of cathodically induced nucleation of copper on nickel and tantalum surfaces.

Proceeding from the fact that bulk silver<sup>3,4</sup> and silver dispersed on a carbon support<sup>5-8</sup> are effective catalysts for the reduction of oxygen in alkaline solutions and that the electrochemical deposition of metals on a titanium surface provides highly developed surfaces,<sup>26-29</sup> an electrochemically formed Ag/TiO<sub>2</sub> composite was selected for detailed study. In continuation of a previous study of this composite formed by a definite program of potentiodynamic polarization,<sup>31</sup> and bear-

ing in mind the possible template action of a TiO<sub>2</sub> layer,<sup>29</sup> an attempt was made to enlarge the possibilities to control both the morphology and the catalytic effectiveness of electrochemically formed layers, by expanding the modes of silver deposition. In both deaerated and oxygen-saturated aqueous 0.1 M NaOH solution, the electrochemical behaviour of the obtained Ag/TiO<sub>2</sub> composite layers was examined and compared to that of a bulk polycrystalline silver electrode.

#### EXPERIMENTAL

The electrochemical cell was a double-walled thermostated glass cell, with the electrodes and gas inlet tube immersed through tight, machined orifices on the plastic top cover. The working electrode support was a rod of titanium 3 mm in diameter, pressed into a PTFE insulating cylinder, being the detachable part of a rotating electrode. The reference electrode was a commercial Beckman saturated calomel electrode (SCE). The counter electrode was a platinum foil. The reference electrode was separated from the bulk electrolyte by a Luggin capillary filled with the investigated electrolyte.

The solutions were made from Merck or Aldrich p.a. chemicals and redistilled water, which were either deaerated by an argon stream or oxygen-saturated by flowing gaseous oxygen. The purity of the gases was 99.999 vol. %.

The dc measurements were performed using a PAR Model 273 Potentiostat/Galvanostat. The rotation speed of the working electrode was controlled by a Beckman rotating electrode device. The electrolyte temperature was always kept at 25 °C.

To prepare the working electrode for electrochemical investigations, the exposed, disk-shaped Ti surface was dry-cleaned with emery paper No. 1200, and plated with silver from a dilute aqueous  $x$  M AgNO<sub>3</sub> + 0.1 M KClO<sub>4</sub> solution, either at a constant potential of -0.4 V vs. SCE, or by potentiodynamic cycling. Simultaneously, a TiO<sub>2</sub> layer was grown either spontaneously, by corrosion<sup>32</sup> or because of potentiodynamic polarization.

The microphotographs of the composite Ag/TiO<sub>2</sub> layers were taken by scanning electron microscope, Jeol JSM-840A.

#### RESULTS AND DISCUSSION

##### *Cyclic voltammetry of freshly polished titanium in aqueous AgNO<sub>3</sub> solutions and the modes of formation Ag/TiO<sub>2</sub> composite layers*

As a valve metal, under usual conditions, titanium is covered by a spontaneously formed semi-conductive oxide layer, which permits electrochemical reduction reactions<sup>33</sup> and suppresses oxidation ones.<sup>34</sup> If formed by anodic oxidation, the thickness of the oxide layer is closely related to the final anodic potential.<sup>32</sup> Electrochemical deposition of any metal on a titanium surface is always influenced by either the spontaneous or electrochemical formation of TiO<sub>2</sub>, diminishing the adherence or directing the sites of preferential electrodeposition.<sup>29</sup> In order to test the conditions of silver deposition from the solution  $1.76 \times 10^{-2}$  M AgNO<sub>3</sub> in 0.1 M KClO<sub>4</sub> as supporting electrolyte, cyclic voltammograms of a freshly polished titanium electrode were recorded in this solution. The potential interval used, *i.e.*, between -0.4 and 0.8 V, as shown in Fig. 1, covers the range of cathodic deposition and anodic dissolution. The first scan reflects both silver

nuclei formation and growth of a  $\text{TiO}_2$  layer. Since  $\text{TiO}_2$  formation was completed within the first anodic sweep, usually not more than three polarization cycles were required to achieve voltammograms of reproducible shape. The voltammograms in Fig. 1 indicate that the reversible potential of a silver electrode in this solution is 0.35 V vs. SCE. Bearing in mind that  $\text{TiO}_2$  does not permit anodic processes on its surface, the pronounced current of anodic dissolution shown in Fig. 1 evidences that most of the deposited silver is in electronic contact with the titanium support. Good contact, providing for both good anodic dissolution and reproducible voltammograms, may be achieved if the starting potential is as close as possible to the open circuit potential of metallic titanium, which is below  $-1$  V in neutral aqueous solutions. Such a negative starting potential may enable silver nuclei to form on almost bare metal surface. Higher starting potentials cause an instantaneous growth of  $\text{TiO}_2$ , the thickness of which is closely correlated to the highest value of the anodic potential.<sup>31,32</sup> The study of Emery *et al.*<sup>30</sup> illustrates the consequences of the formation of such an oxide interlayer. These authors studied copper deposition on tantalum, starting the potentiodynamic polarization from the anodic side of the potential interval they studied. In such a manner, they formed an oxide layer prior to the commencement of electrocrystallisation of copper. In the case of the formation of this oxide layer, copper was easily deposited cathodically and accumulated in each polarization cycle, however, the anodic dissolution was almost completely blocked. In addition, Poroshkov *et al.*<sup>1</sup> reported a significant asymmetry between the current consumptions for the cathodic and anodic processes, in favour of the cathodic process, during silver deposition and dissolution on an anodised Ti surface.

The first type of Ag/ $\text{TiO}_2$  deposit, labelled in this study as composite layer type I, presented in Fig. 2, was prepared by immersing a freshly polished titanium surface in solution  $1.7 \times 10^{-2}$  M  $\text{AgNO}_3$  + 0.1 M  $\text{KClO}_4$ , and instantaneously subjecting it to a constant potential of  $-0.4$  V vs. SCE. According to the voltammograms in Fig. 1, this potential corresponds to the limiting diffusion current of silver deposition from an unstirred solution. However, this potential allows the instantaneous formation of a  $\text{TiO}_2$  film, about 1 nm thick. It is reasonable to expect that various imperfections caused by mechanical polishing and chemical impurities result in non-uniformity in the thickness of the layer in its initial stage of development, whereby nucleation of silver is favoured at the sites covered with a thinner  $\text{TiO}_2$  layer. This causes a non-uniform surface coverage, *i.e.*, favoured sites of silver crystals development or, in other words, a template effect of the  $\text{TiO}_2$  layer. During 30 s of silver deposition, the current increased almost linearly from 0 up to  $1.4 \text{ mA cm}^{-2}$ . According to the Faraday law, it is easy to calculate that the number of coulombs consumed in this procedure generates a surface loading by silver of  $24 \text{ } \mu\text{g cm}^{-2}$ . After this constant potential treatment, one potentiodynamic sweep in the same solution was performed with a ver-

tex anodic potential of 0.3 V, in order to thicken the TiO<sub>2</sub> layer on the silver-free fraction of the titanium surface. The vertex anodic potential was limited in this case to 0.3 V, since, as Fig. 1 shows, at higher potentials anodic dissolution of the deposit may occur.

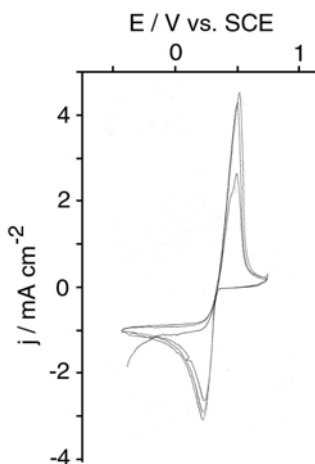


Fig. 1. The cyclic voltammograms of a Ti electrode in  $1.76 \times 10^{-2}$  M AgNO<sub>3</sub> + 0.1 M KClO<sub>4</sub> recorded between -0.4 and 0.8 V at a scan rate of  $50 \text{ mV s}^{-1}$ , with  $E_1 = -0.4 \text{ V}$  and  $E_2 = 0.8 \text{ V}$ , and  $E_3 = E_1 = -0.4 \text{ V vs. SCE}$ .

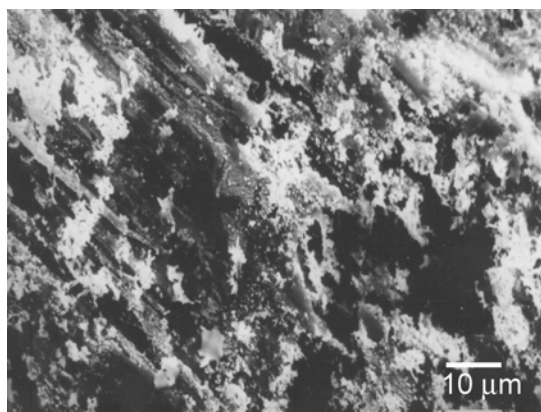


Fig. 2. The SEM microphotograph of a titanium surface with silver cathodically deposited at a constant potential of  $-0.4 \text{ V vs. SCE}$  during 30 s (Ag/TiO<sub>2</sub>, type I).

An SEM photograph of the Ag/TiO<sub>2</sub> surface with potentiostatically deposited silver is shown in Fig. 2. Since the back-scattered electron mode was used, the parts of surface rich in the heavier element, in this case Ag, appear highlighted. Along the surface, a number of randomly distributed silver dots, as well as cotton-like flecks composed of numerous branched silver nano-whiskers may be observed.

The type II composite layer was obtained when a freshly polished Ti electrode in a more dilute  $1.74 \times 10^{-3}$  M AgNO<sub>3</sub> + 0.1 M KClO<sub>4</sub> solution, was subjected to the potentiodynamic polarization program shown in Fig. 3. In this case, compared to Fig. 1, the polarization program emphasizes both the potential of cathodic deposition and that of anodic dissolution. However, the average time of deposition was longer than the average time of dissolution. Based on the voltammetric curves shown in Fig. 1, the working electrode type II was prepared starting the polarization sweep at  $-1 \text{ V vs. SCE}$ , and sweeping the potential within the limits  $-0.8$  and  $0.5 \text{ V}$  at a rate of  $50 \text{ mV s}^{-1}$ .

The vertex cathodic potential of  $-0.4 \text{ V vs. SCE}$  in the program shown in Fig. 3 corresponds, according to Fig. 1, to silver deposition under diffusion limi-

tation, when, as Fig. 2 shows, silver is able to deposit in the form of branched whiskers. However, at vertex anodic potentials of the potentiodynamic sweeps, (0.5 V), massive anodic dissolution occurs, whereby whiskers are primarily removed. However, under potentiodynamic conditions at the chosen vertex anodic potential, anodic dissolution is incomplete and each polarization cycle leaves a new portion of silver. As a result, a rather regular, dot-like, silver deposit imbedded in the TiO<sub>2</sub> layer appears. The mean diameter may be regulated by the number of polarization cycles. The deposit formed after 8 polarization cycles is shown in Fig. 4. For this type of layer, the surface loading by silver may be determined from the distribution density and mean diameter of silver dots by assuming that they are hemispherical in shape.<sup>31</sup> For further comparison with other types of composite layer types, a layer with a silver loading of 6  $\mu\text{g cm}^{-2}$  was used.

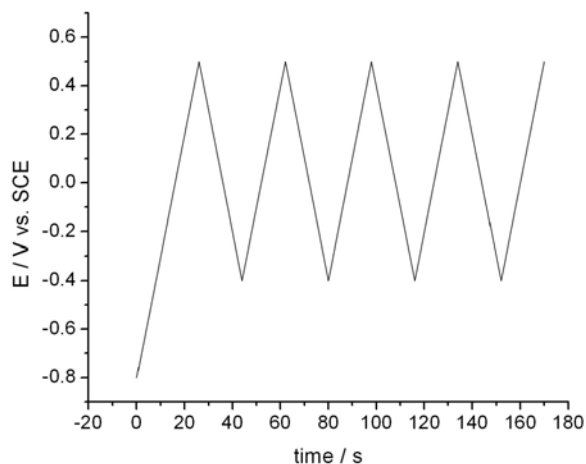


Fig. 3. The program of potentiodynamic polarization by which the Ag/TiO<sub>2</sub> deposit shown in Fig. 4 was obtained.

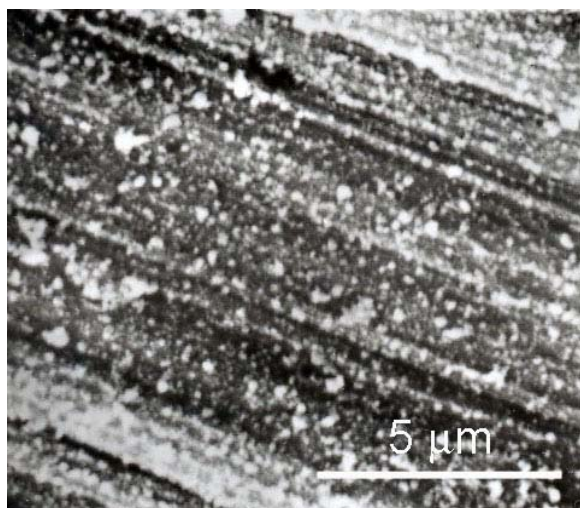


Fig. 4. The SEM microphotograph of a titanium surface upon potentiodynamic deposition of silver, using 8 cycles within the potential limits  $-0.4$  and  $0.5$  V, at a scan rate  $50 \text{ mV s}^{-1}$  (Ag/TiO<sub>2</sub>, type II).

If the polarization program shown in Fig. 5 is applied to a freshly polished titanium surface in  $1.74 \times 10^{-2}$  M AgNO<sub>3</sub> + 0.1 M KClO<sub>4</sub>, with vertex anodic potentials of at least 0.8 V, which provides for almost complete anodic dissolution of silver in each polarization cycle, a new type of deposit appears, labelled as composite layer type III. During each anodic sweep of the polarization cycle, according to Fig. 1, the whiskers grown above the TiO<sub>2</sub> layer during cathodic polarization are subjected to complete anodic dissolution. However, a part of the silver, most probably that screened by the TiO<sub>2</sub> layer growing during anodic polarization, remains protected from anodic dissolution and serves as the sites on which further cathodic deposition is favoured. This explanation is in accordance with the literature,<sup>2</sup> when a notable resistance towards anodic dissolution was reported for silver particles of nanometer dimensions on a graphite support. The SEM picture of the resulting Ag/TiO<sub>2</sub> composite surface is shown in Fig. 6. The silver is placed within randomly distributed micron-sized regions, visible as highlighted areas, integrated in the TiO<sub>2</sub> layer. The silver-rich islands are distributed relatively uniformly over the whole titanium surface and occupy about 50 % of the surface. Using a higher magnification, silver agglomerates approx. 50–150 nm in diameter may be distinguished within these silver-rich regions. The composite layer produced by the above described potentiodynamic procedure appears to be very adherent; namely, it cannot be stripped by strong rubbing with filter paper. This is expectable, since during each polarization cycle when the potentials exceeded 0.4 V, the exposed part of silver deposit, namely that not captured by TiO<sub>2</sub>, is removed by anodic dissolution.

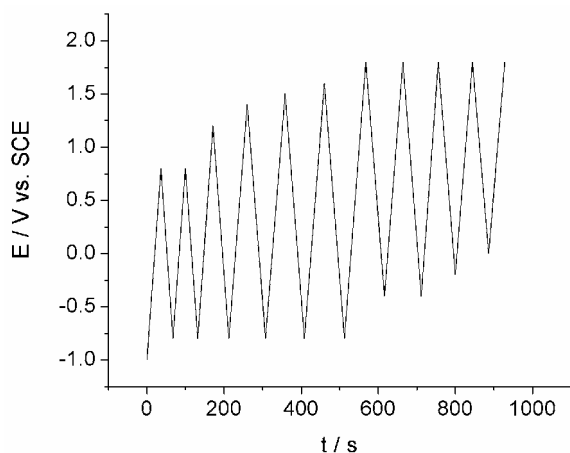


Fig. 5. The potential–time program used for the synthesis of the Ag/TiO<sub>2</sub> layer shown in Fig. 6.

*The cyclic voltammograms of the Ag/TiO<sub>2</sub> composite layers in deaerated alkaline solutions*

In alkaline solutions under anodic polarization, silver does not dissolve anodically but undergoes surface oxidation.<sup>35–37</sup> The redox processes in Ag/Ag<sub>2</sub>O–AgO

systems in alkaline solutions present the fundamentals of silver–zinc alkaline batteries. Numerous papers published previously<sup>35–41</sup> were dedicated to the investigation of electrochemically induced changes on a silver surface in alkaline solutions. Oxidation was found to be a multi-stage process. In the region of surface oxidation, the two main anodic peaks, between 0 and 0.8 V *vs.* SCE correspond to the formation of Ag<sub>2</sub>O and AgO, respectively, the first of which displays a fine structure. The majority of authors agree that the pre-peak which arises at about 0.1 V *vs.* SCE and precedes the formation of Ag<sub>2</sub>O may be attributed to a phase transformation of adsorbed OH<sup>−</sup> into an AgOH layer. The other two peaks, situated between 0.2 V and 0.4 V *vs.* SCE, are due to the formation of compact and porous Ag<sub>2</sub>O layer, respectively.<sup>40,41</sup> Much more cathodic, between −0.5 and −0.8 V *vs.* SCE, at a substantially expanded current scale, a pair of peaks, which were attributed to the adsorption/desorption of OH<sup>−</sup> ions<sup>42</sup> can be discerned. The presence of adsorbed OH<sup>−</sup> ions was recently confirmed by XPS,<sup>43,44</sup> Raman spectroscopy<sup>45</sup> and by electron diffraction.<sup>46</sup>

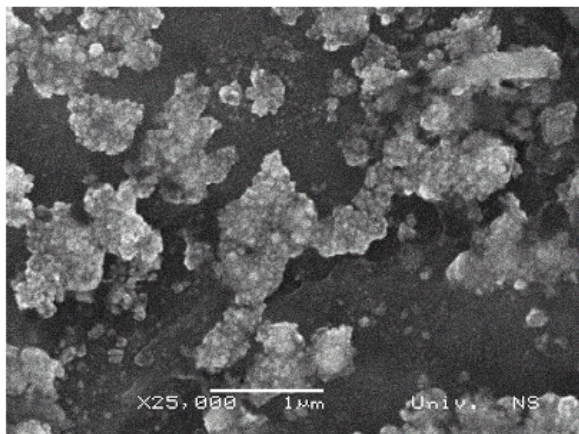


Fig. 6. SEM Microphotographs of Ag/TiO<sub>2</sub> (type III) surface.

To estimate the fraction of silver within the Ag/TiO<sub>2</sub> composite layer, which may be transformed into oxides, a titanium electrode covered by a Ag/TiO<sub>2</sub> layer in perchlorate solution was rinsed with distilled water, transferred into a 0.1 M NaOH solution, and then voltammograms were recorded in the potential range −1.0 to 0.9 V. These voltammograms are presented in Figs. 7 and 8, together with the voltammograms of a bulk polycrystalline silver electrode, which had been abraded in the same manner as the titanium one, supporting the Ag/TiO<sub>2</sub> layer.

The voltammogram of bulk polycrystalline silver (the second polarization cycle is presented) displays two well-known main anodic peaks. The second one of these two oxidation peaks, if a slow polarization rate is used, may be completely separated from the current of oxygen evolution.<sup>38,42</sup> However, in the present case these processes are somewhat merged. For this reason, the cathodic peaks appear to be more representative to estimate the charge consumed for the forma-

tion of surface oxides. In Fig. 7, for polycrystalline silver, the surface of the higher cathodic peak corresponds to a surface charge density of  $129 \text{ mC cm}^{-2}$ , which, assuming  $\text{Ag}_2\text{O}$  reduction corresponds to a further coverage by silver of  $144 \mu\text{g cm}^{-2}$ . Other authors found that a charge of  $130 \text{ mC cm}^{-2}$  might be consumed for oxide formation,<sup>20</sup> which is very similar to the value found here. To estimate the thickness of a silver surface layer, expressed as the number of atomic layers, which participates in oxide formation, the number of atoms within one atomic layer has to be known. Horswell *et al.*<sup>46</sup> reported that the number of silver atoms per square centimeter for low-index planes of an Ag monocrystal amounts on average to  $10^{15}$ . The above-mentioned value of  $129 \text{ mC cm}^{-2}$  corresponds to roughly  $8 \times 10^{17}$  silver atoms per square centimetre of geometric surface area. Thus, taking into account a roughness factor of between 1 and 3 for polycrystalline silver abraded with emery paper and bearing in mind the average number of atoms in one surface atomic layer,<sup>46</sup> it is reasonable to assume that several hundreds of atomic layers on the surface of a bulk silver electrode participate in metal oxide conversion reactions.

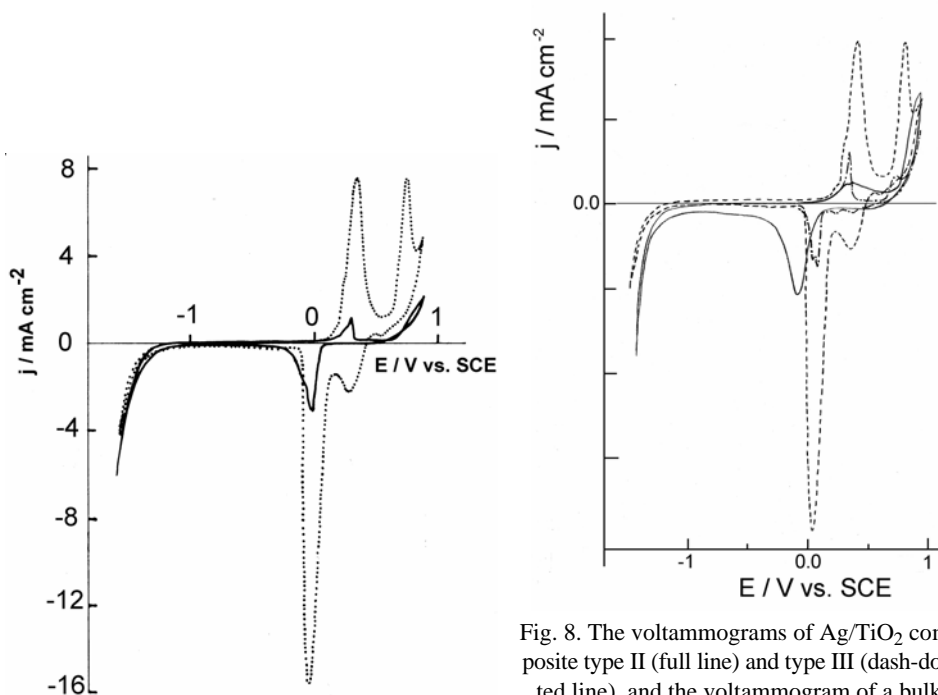


Fig. 7. The voltammogram of an Ag/TiO<sub>2</sub> type I layer (full line) and the voltammogram (second scan) of bulk polycrystalline Ag (dotted line), recorded in 0.1 M NaOH between  $-1.6$  and  $0.9 \text{ V vs. SCE}$ , at a scan rate  $20 \text{ mV s}^{-1}$ .

Fig. 8. The voltammograms of Ag/TiO<sub>2</sub> composite type II (full line) and type III (dash-dotted line), and the voltammogram of a bulk silver electrode in argon-purged 0.1 M NaOH, at a scan rate  $20 \text{ mV s}^{-1}$ . The unit of current density axis is 4.0, 0.4 and  $1.0 \text{ mA cm}^{-2}$ , for the bulk silver, composite layer type II and composite layer type III, respectively.

For Ag/TiO<sub>2</sub>, type I layer, in Fig. 7, the surface area of the cathodic peak is about 5.4 times lower than that of an activated bulk silver electrode, and corresponds to a surface loading by silver of 25.7  $\mu\text{g cm}^{-2}$ . Bearing in mind that a loading by silver of 24  $\mu\text{g cm}^{-2}$  was calculated on the basis of the electricity consumed for the synthesis of this composite layer, it may be concluded that, within experimental error, the silver involved in the surface of an Ag/TiO<sub>2</sub> type I composite layer may be converted completely into oxide.

For Ag/TiO<sub>2</sub> type II and III layer, in Fig. 8, the charge density which corresponds to oxide reduction amounts to 4.9 and 3  $\text{mC cm}^{-2}$ , respectively. The value 4.9  $\text{mC cm}^{-2}$  corresponds to 5.4  $\mu\text{g cm}^{-2}$ , which is reasonably close to the 6  $\mu\text{g cm}^{-2}$  calculated based on the SEM picture (Fig. 4, top). Returning to the Ag/TiO<sub>2</sub> electrode type III, the value of 3  $\text{mC cm}^{-2}$  for the main reduction peak corresponds to a silver loading of 3.4  $\mu\text{g cm}^{-2}$ . This value is also far lower than that (130  $\text{mC cm}^{-2}$ ) consumed to oxidize the bulk silver surface and, therefore, it may be assumed that this is the silver loading responsible for the catalytic activity of this layer.

*The voltammograms of the Ag/TiO<sub>2</sub> composite layers in oxygen-saturated alkaline solutions*

Bulk polycrystalline platinum, carbon-supported platinum<sup>47</sup> and platinum alloys<sup>48,49</sup> display admirable catalytic activity towards the oxygen reduction reaction, ORR, in both acidic and alkaline solutions and thus present the unavoidable candidate for practical application in low temperature fuel cells. Many years ago, Tarasevich *et al.*<sup>3</sup> published that in alkaline solutions only, silver displays a catalytic activity for the ORR comparable to that of platinum. Based on this knowledge, some authors recently investigated the possibility of developing a carbon-supported silver catalyst for oxygen reduction in alkaline solutions.<sup>5-9</sup> The present study follows this trend using another type of supporting material, namely titania covered titanium, and a different electrochemical procedure of synthesis.

The voltammograms of the ORR on an Ag/TiO<sub>2</sub> rotating disc in 0.1 M NaOH oxygen-saturated solutions are presented in Fig. 9. According to Figs. 7 and 8, in the voltage region given in Fig. 9, the silver surface is free of silver oxide. However, in a part of this voltage region, namely that between -0.8 and 0.0 V, according to observations by very sensitive methods,<sup>42-45</sup> the silver is covered by adsorbed OH<sup>-</sup> ions. The voltammograms in Fig. 9 indicate that the ORR proceeds easily on the composite surfaces under investigation and attains diffusion limitation over a large voltage interval. Mentus<sup>31</sup> published that the ORR also proceeds on anodic TiO<sub>2</sub> alone. However, in comparison to even extensively activated TiO<sub>2</sub>,<sup>50</sup> a much lower overvoltage is required to run the ORR on Ag/TiO<sub>2</sub> than on pure TiO<sub>2</sub>. It is thus certain that silver plays the main role in the acceleration of the ORR on Ag/TiO<sub>2</sub> composite layers.

The voltammograms from Fig. 9 were transformed into Tafel plots, which are shown in Fig. 10. The correction for the diffusion current consisted in the fac-

tor  $j_l/(j_l-j)$ , where  $j_l$  is the limiting diffusion current.<sup>8,9</sup> For the sake of comparison, the Tafel curves for the ORR on the surface of activated bulk polycrystalline silver is also presented.

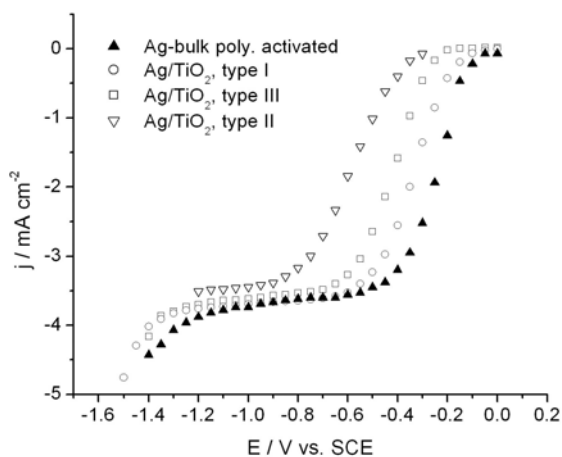


Fig. 9. The voltammograms of the oxygen reduction on various Ag/TiO<sub>2</sub> composite deposits on a rotating Ti disc electrode in oxygen saturated 0.1 M NaOH solutions, at a common rotation rate of 10 rps.

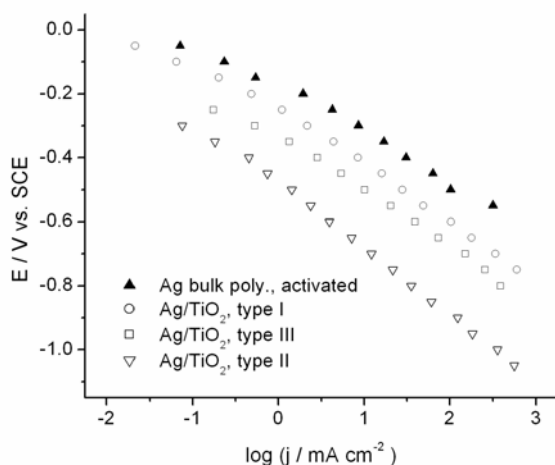


Fig. 10. Tafel plot of oxygen reduction on various Ag/TiO<sub>2</sub> composite deposits and bulk polycrystalline silver in oxygen-saturated aqueous 0.1 M NaOH solutions.

The Tafel slopes in Fig. 10 range between the lowest one of 100 mV for activated bulk silver (which is very similar to the slope found by Bliznac<sup>51</sup> for an Ag(100) surface in 0.1 M KOH) to the highest 200 mV per decade for the type II composite Ag/TiO<sub>2</sub> surface for higher current densities, cds. Assuming the rate controlling step is  $O_2 + e^- = O_2^-$ , the expected Tafel slope should amount to -60 mV per decade and such a slope was observed with platinum and some other noble metals in the low current density range.<sup>52</sup> However, usually a transition in slope from -60 to -120 mV per decade was observed on going from the low current density (lcd) towards the high current density (hcd) region. This transition was explained in terms of a transition from Temkin to Langmuir conditions caused by

a drop to zero in the surface coverage of adsorbed oxygen,<sup>52</sup> not in change in the nature of the rate determining step. Regarding silver, from both a previous<sup>51</sup> and this study, it seems that the low current density range of oxygen reduction, like that observed with a platinum electrode, is completely absent. A feature connected to the ORR on an Ag/TiO<sub>2</sub> surface is the larger Tafel slope in comparison to bulk silver. Thus, it seems that Ag/TiO<sub>2</sub> displays generally an averaged behaviour between that of pure silver and that of pure TiO<sub>2</sub>. The same behaviour was evidenced elsewhere in the case of a Pt/TiO<sub>2</sub> catalyst, for low metal loadings.<sup>53</sup>

In alkaline solutions, the oxygen reduction reaction proceeds on different electrode materials usually as a direct, 4e<sup>-</sup> reaction or as an indirect, 2e<sup>-</sup> reaction,<sup>58</sup> whereby the latter one is accompanied and detectable by peroxide ion liberation from the electrode surface. A rotating disc–ring electrode presents a powerful tool to distinguish easily between these two reaction paths. Using the ring–disc method, Blizanac<sup>51</sup> evidenced that the oxygen reduction reaction for compact monocrystalline silver electrodes in alkaline solutions always proceeds through a 4e<sup>-</sup> path. To prove the possible reaction path on the various Ag/TiO<sub>2</sub> composite layers, the results of rotating disc experiments were analysed using current–potential plots recorded at various rotation rates.

For a diffusion limited electrochemical reaction on rotating disc electrode, the current density follows the linear dependence on the square root of the rotation frequency, as predicted by the Levich equation:

$$j_1 = 0.62nFD^{2/3}\nu^{-1/6}\omega^{1/2}c \quad (1)$$

This may be written in its shorter form:

$$j_1 = B\omega^{1/2} \quad (1')$$

where  $\nu$  presents the kinematic viscosity, *i.e.*, the viscosity divided by density, and  $\omega$  is the angular rotation frequency ( $\omega = 2\pi f$ , where  $f$  is the rotation frequency). The kinematic viscosities of the dilute perchlorate solutions used here are very close to that of water and thus may be taken to amount to 0.01 cm<sup>2</sup> s<sup>-1</sup>. The disc current density of any mixed activation–diffusion controlled process, at a fixed potential, follows the Koutecky–Levich (K–L) plot:<sup>54</sup>

$$\frac{1}{j} = \frac{1}{j_\infty} + \frac{1}{B\omega^{1/2}} \quad (2)$$

The meaning of  $B$  is visible from Eqs. (1) and (1'), while  $j_\infty^{-1}$  is the intercept on the ordinate at infinite rotation frequency.

For dilute, oxygen-saturated solutions,  $B$  depends exclusively on the number of electrons,  $n$ , consumed per one oxygen molecule and for  $n = 4$  amounts to 0.432 mA cm<sup>-2</sup> s<sup>1/2</sup>, while for  $n = 2$ , it is 0.216 mA cm<sup>-2</sup> s<sup>1/2</sup>.

The K–L slopes obtained for the studied composites are compared to that for a monocrystalline Ag(100) surface<sup>51</sup> in Fig. 11. In all cases observed in this study, as Fig. 11 shows, the K–L slopes were very close to that found with Ag(100) monocrystalline surface, which definitely corresponds to a 4e<sup>-</sup> reaction path.<sup>51</sup> This is an expected result, since both Ag<sup>51</sup> and TiO<sub>2</sub>,<sup>50</sup> support a 4e<sup>-</sup> path in alkaline solutions.

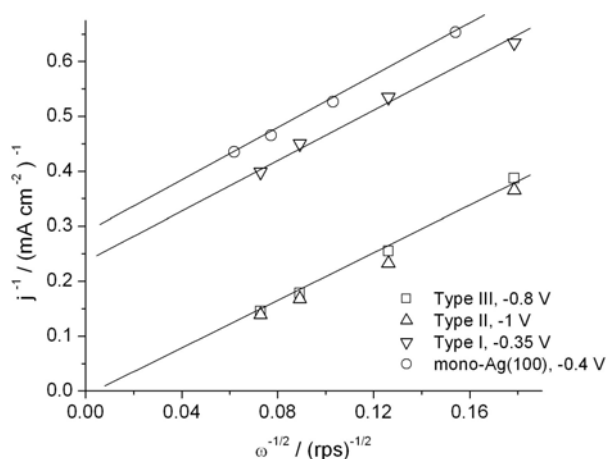


Fig. 11. Koutecky–Levich plot for the oxygen reduction reaction on different types of Ag/TiO<sub>2</sub> composite layers, compared to literature data for Ag(100) in 0.1 M NaOH.<sup>51</sup>

The value of the current density at a common overvoltage may be used as a measure of catalytic activity. For a fixed potential of  $-0.3$  V vs. SCE, from Fig. 10, the current readings are 0.079, 0.50, 2.0 and 8.9 mA cm<sup>-2</sup>, for composites with a silver loading 6.0, 3.4, 24  $\mu\text{g cm}^{-2}$ , and activated bulk silver, respectively. The increase in catalytic activity follows generally the loading by silver. However, the inversion, appearing in the range of the lowest loadings, indicates also the influence of the mode of surface preparation. Namely better activity was observed with the composite layer in which a better degree of integration of silver into TiO<sub>2</sub> was achieved (Fig. 6 vs. Fig. 4). This inversion may be taken as evidence of a synergistic effect in the observed system.

It would be more exact to correlate the catalytic effectiveness to the number of surface silver atoms (*i.e.*, the real silver surface area), being a more fundamental parameter of catalysis than surface loading. However, to date, there is no reliable method for the determination of the real surface area of a silver electrode, such as that developed for platinum based on hydrogen electrosorption,<sup>47</sup> or that developed for gold based on oxygen electrosorption.<sup>55</sup> Namely, the amount of OH<sup>-</sup> ions adsorbed on a silver surface in the potential range  $-0.8$  to  $-0.5$  V vs. SCE<sup>44–46</sup> does not achieve a plateau, characteristic of monolayer formation<sup>46</sup> and, with further anodic polarization, passes rather continuously into oxide formation, while the oxide formation itself is multilayer in nature.<sup>39–41</sup>

The fair catalytic activity of the Ag/TiO<sub>2</sub> layer at relatively small surface loadings of only 3.4–6 and 24 μg cm<sup>-2</sup> may be the result of some combined effects connected to the dispersed structure of the silver deposit. Recently, several authors reported on the importance of disorder of the surface atoms or atom clusters as being essential for catalytic activity.<sup>56–58</sup> Namely, a surface layer often consists of atoms and clusters in metastable states, which are difficult to generate in a reproducible manner.<sup>57,58</sup> This concept of metastable surfaces may be interrelated to surface reconstructions.<sup>59,60</sup> Using both the thickness of anodic surface oxides and the dependence of voltammograms on the type of electrode pre-treatment (Figs. 7 and 8), as a measure of surface metastability, silver may be classified to metals the surface of which is easily transferred into metastable states. The developed morphology of silver within the Ag/TiO<sub>2</sub> composite layer allows a great number of disordered surface atoms, as well as a pronounced synergy.

#### CONCLUSIONS

Proceeding from the fact that a thin TiO<sub>2</sub> film, if formed on a Ti surface simultaneously with the cathodic formation of metal nuclei, may template metal nuclei distribution, the forms Ag/TiO<sub>2</sub> deposits obtained either by potentiostatic or potentiodynamic polarization of a freshly polished titanium surface in dilute aqueous solutions of silver nitrate were investigated. The SEM micrographs indicate that branchy silver whiskers crossing the TiO<sub>2</sub> layer were obtained by potentiostatic deposition, while dot-like and island-like silver deposits integrated in the TiO<sub>2</sub> layer were obtained by potentiodynamic polarization. By comparing the cyclic voltammograms of composite Ag/TiO<sub>2</sub> electrodes to a bulk Ag electrode in deaerated 0.1 M NaOH solution, it was concluded that all the silver in an Ag/TiO<sub>2</sub> layer could be converted to oxide. Consequently, cyclic voltammetry was used for coulometric determination of the surface loading by silver. The surface loading, determined in such a way, corresponded well to the one determined by other methods used, based either on the current consumption during potentiostatic deposition, or on SEM analysis.

The catalytic activity of Ag/TiO<sub>2</sub> layers toward oxygen reduction reaction was investigated in oxygen saturated alkaline 0.1 M NaOH. Fair electrocatalytic activity was evidenced for very small loadings of silver of the order 10<sup>-6</sup> g cm<sup>-2</sup>. As expected, the catalytic activity increases with increasing silver loading. A registered deviation of this rule evidenced the role of silver integration into TiO<sub>2</sub>.

By the Koutecky–Levich analysis, a 4e<sup>-</sup> reaction path of oxygen reduction, characteristic of bulk silver in alkaline solutions, was confirmed for all the studied Ag/TiO<sub>2</sub> composite layers.

*Acknowledgements.* One of the authors (S. M) is participant in the EU Project “Prometeas”, Contract No. ICA2-CT-2001-10037 and in the contract No. 142047 agreed with the Ministry of Science of the Republic of Serbia. The authors S. M, I. B, J. P. and V. G. are grateful to the Ministry of Education and Science of the Republic of Montenegro which supported this work through contract No. 05-1/2-1530/2005.

## ИЗВОД

ПОДЕШАВАЊЕ МОРФОЛОГИЈЕ И ЕЛЕКТРОКАТАЛИТИЧКИХ СВОЈСТАВА  
ЕЛЕКТРОХЕМИЈСКИ ФОРМИРАНОГ КОМПОЗИТНОГ СЛОЈА Ag/TiO<sub>2</sub>  
НА ПОВРШИНИ ТИТАНАС. В. МЕНТУС<sup>1</sup>, И. БОШКОВИЋ<sup>2</sup>, Ј. М. ПЕШЧИЋ<sup>2</sup>, В. ГРУДИЋ<sup>2</sup> И Ж. БОГДАНОВ<sup>3</sup><sup>1</sup>Факултет за физичку хемију, Универзитет у Београду, Студентски Трз 16, 11000 Београд, <sup>2</sup>Универзитет у  
Подгорици, Металуршко-технолошки факултет, 81000 Подгорица, Црна Гора и<sup>3</sup>Институт за нуклеарне науке "Винча", 11001 Београд

У воденом раствору AgNO<sub>3</sub>, подешавајући услове издвајања сребра на површини механички полираног титана, добијене су три различите форме композитног слоја Ag/TiO<sub>2</sub>, у којима депозит сребра има облик иглица, тачака и острвца. Морфологија депозита је резултат програма поларизације електроде и усмеравајућег (темплатног) дејства слоја TiO<sub>2</sub> који се формира паралелно са издвајањем сребра. Каталитичка активност композитних депозита према редукцији кисеоника испитивана је у воденом раствору 0,1 М NaOH. Показано је да она зависи од количине и типа дистрибуције сребра унутар слоја Ag/TiO<sub>2</sub>. Независно од форме композита, реакциони пут редукције кисеоника је четвороелектронски, иначе карактеристичан за поликристално сребро у алкалном раствору.

(Примљено 14. маја 2007)

## REFERENCES

1. V. P. Poroshkov, V. S. Gurin, *Surf. Sci.* **331–333** (1995) 1520
2. K. H. Ng, H. Liu, R. M. Penner, *Langmuir* **16** (2000) 4016
3. N. A. Shumilova, G. N. Zhutaeva, M. R. Tarasevich, *Electrochim. Acta* **11** (1967) 967
4. J. D. McIntyre, W. F. Peck, in: *The Physics and Chemistry of Electrocatalysis*, J. D. E. McIntyre, M. J. Weaver, E. Yeager, Eds., Pennington, N.Y., 1984, p. 102
5. V. Hacker, E. Wallöfer, W. Baumgartner, T. Schaffer, J. O. Besenhard, H. Schröttner, M. Schmid, *Electrochem. Commun.* **7** (2005) 377
6. Y.-F. Yang, Y.-H. Zhon, *J. Electroanal. Chem.* **397** (1995) 271
7. Y.-F. Yang, Y.-H. Zhon, *J. Electroanal. Chem.* **415** (1996) 143
8. M. Chatenet, L. Genies-Bultel, M. Aurousseau, R. Durand, F. Andolfatto, *J. Appl. Electrochem.* **32** (2002) 1131
9. M. Chatenet, M. Aurousseau, R. Durand, F. Andolfatto, *J. Electrochem. Soc.* **150** (2003) D47
10. S. Gamburgzev, K. Petrov, A. J. Appleby, *Book of Abstracts, in Proceedings of Joint Meeting – 200<sup>th</sup> Meeting of ECS, Inc., and 52<sup>nd</sup> Ann. Meeting of ISE*, San Francisco, California, 2001, Abst. No. 353
11. R. R. Adžić, J. X. Wang, *Electrochim. Acta* **45** (2000) 4203
12. S. J. Tauster, S. C. Fung, R. T. K. Baker, J. A. Horsley, *Science* **211** (1981) 1121
13. G. L. Haller, D. E. Resasco, *Adv. Catal.* **36** (1989) 173
14. B. C. Beard, P. N. Ross, *J. Electrochem. Soc.* **133** (1986) 1839
15. S. G. Neophytides, S. H. Zafeiratos, M. M. Jaksic, *J. Electrochem. Soc.* **150** (2003) E512
16. M. Haruta, S. Tsubota, T. Kobayashi, H. Kageyama, M. J. Genet, B. Delmon, *J. Catal.* **144** (1993) 175
17. G. R. Bamwenda, S. Tsubota, T. Nakamura, M. Haruta, *Catal. Lett.* **44** (1997) 83
18. M. Okumura, K. Tanaka, A. Ueda, M. Haruta, *Solid State Ionics* **95** (1997) 143
19. S. Trasatti, in: *Interfacial Electrochemistry, Theory, Experiment and Applications*, A. Wieckowski Ed., M. Dekker Inc., New York, 1999, p. 769

20. H. B. Beer, *J. Electrochem. Soc.* **127** (1980) 303C
21. S. Tsubota, D. A. H. Cunningham, Y. Baudo, M. Haruta, *Preparation of Catalysts* **6** (1995) 227
22. J. R. Burrows, J. H. Eutwisle, J. A. Harrison, *J. Electroanal. Chem.* **77** (1977) 21
23. A. T. Kuhn, C. J. Mortimer, *J. Electrochem. Soc.* **12** (1973) 231
24. E. A. Kalinovskii, R. V. Boudar, N. N. Meshkova, *Elektrokhimiya* **8** (1972) 1468
25. R. G. Erenberg, L. J. Krishtalik, V. J. Bystrov, *Elektrokhimiya* **8** (1972) 1740
26. D. Čukman, M. Vuković, *J. Electroanal. Chem.* **279** (1990) 273
27. D. Čukman, M. Vuković, M. Milun, *J. Electroanal. Chem.* **389** (1995) 209
28. M. Vuković, D. Marijan, D. Čukman, P. Pervan, M. Milun, *J. Mat. Sci.* **34** (1999) 869
29. S. Mentus, *Electrochim. Acta* **50** (2005) 3609
30. S. B. Emery, J. L. Hubbey, D. Roy, *J. Electroanal. Chem.* **568** (2004) 121
31. I. Bošković, S. V. Mentus, M. Pješčić, *Electrochim. Acta* **51** (2006) 2793
32. J. Pješčić, S. Mentus, N. Blagojević, *Mater. Corros.* **53** (2002) 44
33. R. M. Torresi, O. R. Camara, C. P. DePauli, M. C. Giordano, *Electrochim. Acta* **32** (1987) 1357
34. S. K. Poznyak, A. I. Kokorin, A. I. Kulak, *J. Electroanal. Chem.* **442** (1998) 99
35. B. V. Tilak, R. Perkins, H. A. Kozłowska, B. E. Conway, *Electrochim. Acta* **17** (1972) 1447
36. R. S. Perkins, B. V. Tilak, H. A. Kozłowska, *Electrochim. Acta* **17** (1972) 1471
37. J. M. M. Droog, P. T. Alderliesten, G. A. Bootsma, *J. Electroanal. Chem.* **99** (1979) 173
38. M. Hepel, M. Tomkiewicz, *J. Electrochem. Soc.* **131** (1984) 1288
39. M. L. Teijelo, J. R. Vilche, A. J. Arvia, *J. Appl. Electrochem.* **18** (1988) 691
40. B. M. Jović, V. D. Jović, G. R. Stafford, *Electrochem. Commun.* **1** (1999) 247
41. B. M. Jović, V. D. Jović, *J. Serb. Chem. Soc.* **69** (2004) 153
42. G.I. Lacconi, A.S. Gioda, V.A. Macagno, *Electrochim. Acta* **30** (1985) 211
43. D. Hecht, H.H. Strehblow, *J. Electroanal. Chem.* **440** (1997) 211
44. D. Lutzenkirchen–Hecht, H.H. Strehblow, *Electrochim. Acta* **43** (1998) 2957
45. E. R. Savinova, P. Kraft, B. Pettinger, K. Doblhofer, *J. Electroanal. Chem.* **430** (1997) 47
46. S. L. Horswell, A. L. N. Pinheiro, E. R. Savinova, M. Danckwerts, B. Pettinger, M.–S. Zei, G. Ertl, *Langmuir* **20** (2004) 10970
47. T. J. Schmidt, H. A. Gasteiger, G. D. Stab, P. M. Urban, D. M. Kolb and R. J. Behm, *J. Electrochem. Soc.* **95** (1998) 2354
48. A. L. N. Pinheiro, A. O. Neto, E. C. de Souza, J. Perez, V. A. Paganin, E. A. Ticianelli and E. R. Gonzales, *J. New Mat. Electrochem. Sys.* **6** (2003) 1
49. U. A. Paulus, A. Wokaun, G. G. Scherer, T. J. Schmidt, V. Stamenković, N. M. Marković, P. N. Ross, *Electrochim. Acta* **47** (2002) 3787
50. T. Clark, D. C. Johnson, *Electroanal.* **9** (1997) 273
51. B. Blizanac, *PhD Thesis*, Faculty of Physical Chemistry, Belgrade University, 2004 (in Serbian)
52. J. O'M. Bockris, S. U. M. Khan, *Surface Electrochemistry, A Molecular Level Approach*, Plenum Press, New York, London, 1993, p. 331
53. M. I. Rojas, M. J. Esplandiú, L. B. Avallé, E. P. M. Levia, V. A. Macagno, *Electrochim. Acta* **43** (1998) 1785
54. K. Tammeveski, T. Tenno, A. Rosental, P. Talonen, L.–S. Johansson, L. Niinistö, *J. Electrochem. Soc.* **146** (1999) 669
55. D. A. J. Rand, R. Woods, *J. Electroanal. Chem. Interf. Electrochem.* **31** (1971) 29
56. G. A. Somorjai, *Chem. Rev.* **96** (1996) 1223
57. M. S. Spencer, *Nature* **323** (1986) 685
58. L. D. Burke, *Gold Bull.* **37** (2004) 125
59. D. M. Kolb, *Prog. Surf. Sci.* **109** (1989) 51
60. A. Henglein, *Ber. Bunsenges. Phys. Chem.* **101** (1997) 1562.